

Cold atoms in optical lattices: a Hamiltonian ratchet

T.S. Monteiro, P.A. Dando, N.A.C. Hutchings, and M. R. Isherwood

Department of Physics and Astronomy, University College London, Gower Street, London WC1E 6BT, U.K.

(Dated: November 20, 2018)

We investigate a new type of quantum ratchet which may be realised by cold atoms in a double-well optical lattice which is pulsed with unequal periods. The classical dynamics is chaotic and we find the classical diffusion rate D is asymmetric in momentum up to a finite time t_r . The quantum behaviour produces a corresponding asymmetry in the momentum distribution which is ‘frozen-in’ by Dynamical Localization provided the break-time $t^* \geq t_r$. We conclude that the cold atom ratchets require $Db/\hbar \sim 1$ where b is a small deviation from period-one pulses.

PACS numbers: 32.80.Pj, 05.45.Mt, 05.60.-k

Cold atoms in optical lattices provide an excellent experimental demonstration of the phenomenon of *Dynamical Localization* [1]. Dynamical Localization (DL) has been described as the so-called ‘quantum suppression of classical chaos’. More precisely, in the usual realizations, a periodically-driven or kicked system is associated with classically chaotic dynamics for sufficiently strong perturbation. Its average energy grows diffusively and without limit, whereas for the corresponding quantum system the diffusion is suppressed after an \hbar -dependent timescale, the ‘break-time’ t^* . The final quantum momentum distribution is localized with a characteristic exponential profile. The formal analogy established with Anderson Localization [2] forms a key analysis of this phenomenon.

A series of recent experiments on Cesium atoms [3] gave a classic demonstration of this effect for atoms in driven or pulsed lattices of sinusoidal form. The possibility of experiments with asymmetric lattices, in particular with asymmetric double wells [4, 5], leads us to investigate the possibility of constructing a ‘clean’ atomic ratchet, where the transport results purely from the chaotic Hamiltonian dynamics, with no Brownian or dissipative ingredients.

There is already an extensive body of work on Brownian ratchets [6], driven by the need to understand biological systems such as molecular motors and certain mesoscopic systems. Some of this work encompasses the quantum dynamics [7]. However, to date there has been very little work on Hamiltonian ratchets. One notable exception is the work by Flach *et al* [8] where the general form of the spatial and temporal desymmetrization required to generate transport was investigated. To our knowledge, the only substantial study of *quantum* Hamiltonian ratchets to date, however, is the work of Dittrich *et al* [9] which concluded that transport occurs in mixed phase-spaces. They demonstrated that overall transport (in their system with periodic boundary conditions) is zero if starting conditions cover all regions of phase-space (including stable islands and chaotic regions) uniformly. A key result was a sum rule which exploited the fact that transport in the chaotic manifold is balanced by transport in the adjoining regular manifolds (stable islands/tori). Very recently [10], it was shown that a kicked map with a ‘rocking’ linear potential leads to confinement

in the chaotic region between a pair of tori which are not symmetrically located about $p = 0$.

Here we propose a new type of Hamiltonian quantum ratchet which, classically, is completely chaotic. This ratchet is consistent with the rules established by Dittrich *et al*, but relies on a different mechanism: the transport is due to a non-uniform momentum distribution within a completely chaotic phase-space. To our knowledge, this is the only example of a clean, non-dissipative ratchet which does not rely on specific dynamical features such as a particular set of islands/tori.

The basic mechanism is as follows: for a repeating cycle of kicks, of strength K_{eff} , perturbed from period-one by a small parameter b , we find that the *classical* diffusion rates for positive and negative momenta (D^+ and D^- respectively) are different up to a finite time. Up to this time, an asymmetry in the classical momentum distribution $N_{cl}(p)$ accumulates with kick number. Beyond this ‘ratchet’ time, t_r , the rates equalize, we have $D^+ \sim D^- \sim D$ (where $D \sim K_{eff}^2/\hbar$ is the total diffusion rate), no more asymmetry accumulates and the net classical momentum $\langle p_{cl} \rangle$ becomes constant. But $\langle p_{cl}^2 \rangle$, of course, continues to grow with time as $\sim Dt$. We find that the corresponding quantum current depends on t^*/t_r : if the break time is too short no asymmetry in the quantum $N_{qm}(p)$ accumulates and there is no quantum transport. If $t^* \gg t_r$ the localization length L becomes large and the effective quantum momentum asymmetry $\sim \langle p_{qm} \rangle / L$ decreases. We find that $t_r \sim \frac{1}{b^2 D}$. A quantum ratchet will have the clearest experimental signature if $t^* \sim t_r$. Since $t^* \sim D/\hbar^2$, our main conclusion is that optimal cold atom ratchets need $Db/\hbar \sim 1$ with small $b < 0.2$.

Here we consider a system with a Hamiltonian given by $H = \frac{p^2}{2} + KV(x) \sum_{n,i} \delta(t - nT_i)$. We model the double-well ratchet potential as $V(x) = \{\sin x + a \sin(2x + \Phi)\}$. In the usual realization of DL, the Quantum Kicked Rotor (QKR), the pulses or kicks are equally spaced. For the ratchet, we introduce a repeating cycle of N unequally spaced kicks, ie $T_1, T_2..T_N$.

The time-evolution operator for the i -th kick of the n -th cycle factorises into a free and a ‘kick’ part $U_i = U_i^{free} U_i^{kick}$.

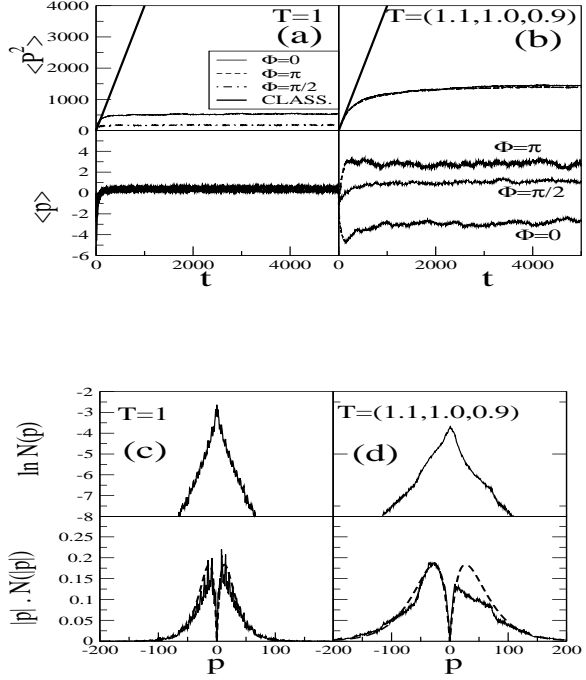


FIG. 1: Effect of equal and unequal kick spacings on a minimal uncertainty gaussian wavepacket with $\hbar = 1/2$ with initial $\langle p \rangle = 0$, for kick strength $K = 2$ and $a = 1/2$, for different Φ . (a) Shows evolution of energy and momentum for $T=1$ (dw-QKR) (b)Shows evolution of energy and momentum for a repeating $N = 3$ cycle of kicks with $b = 0.1$, hence $T_i = 1.1, 1.0, 0.9$ (cdw-QKR). Figs (a) and (b) show that the quantum break time is substantially longer for the unequal kicks. In (b) we illustrate our finding that the classical diffusion rate in the chirped case is very well fitted by the lowest order approximation $D_0 \sim K_{eff}^2/2 \sim 4$ where $K_{eff}^2 = K^2(1 + 4a^2)$ for $D \simeq 2$ or larger. They also show that there is no transport for the equal kick case, but that there is a substantial net momentum ($\sim cst$ if $t > t^*$) for the cdw-QKR. Figs. (c) and (d) show corresponding quantum momentum distributions for the dw-QKR and the cdw-QKR. The figures show that while the logarithmic distribution takes the usual triangular form for the dw-QKR, for the cdw-QKR an asymmetric distribution results. In the lower figure we plot the first moment of the momentum distribution: (to ease comparison we use $|p|$). The net momentum is the difference in area between the positive p and negative p regions. The DL form $|p| \cdot N(|p|) = \frac{|p|}{2L} \exp -|p|/L$ (with $L = 27.5 \sim 3.5D_0/\hbar$ (see fig.3)) is superposed, illustrating that the DL form gives excellent agreement for all cases for large enough p .

In the usual plane wave basis, for a given quasi-momentum q , the matrix elements of U_i can be shown to take the form:

$$U_{ml}^{(i)}(q) = e^{-i\frac{\hbar T_i(l+q)^2}{2}} \sum_s e^{is\Phi} J_{l-m-2s}(\frac{K}{\hbar}) J_s(\frac{aK}{\hbar}) \quad (0.1)$$

where the J are ordinary Bessel functions. The time evolution operator for one period $U(T = \sum_i T_i) = \prod_{i=1}^{i=N} U_i$. In the experiments, an important parameter

is an effective $\hbar_{eff} = 8\omega_r T$ where ω_r is the recoil frequency. In [3], $\hbar_{eff} \sim 1$, so here we have considered the range $\hbar = 1 \rightarrow 1/10$. We can use a re-scaled time such that, without loss of generality, we take the average over the periods in each cycle to unity $\langle T_i \rangle = 1$. We define our ‘chirped’ kicks to mean that we have a repeating cycle of kicks separated by time intervals $1 + nb, 1 + (n-1)b, \dots, 1 - (n-1)b, 1 - nb$ where $n > 0$ is an integer and b is a small time increment. $N = 2n + 1$ for N odd and $N = 2n$ for N even. In particular, our $N = 3$ cycle corresponds to a repeating set of kick spacings $T_1 = 1 + b, T_2 = 1, T_3 = 1 - b$ while an $N = 2$ cycle corresponds to $T_1 = 1 + b, T_2 = 1 - b$ and so forth.

In Fig.1 we compared the evolution of a quantum wavepacket with equal kick times ($T_i = 1$) with a corresponding unequal-kick case with $N = 3, b = 0.1$. Since $V(x)$ in general represents a double well potential, we refer to it as the dw-QKR to distinguish it from the standard map case with $V = K \sin x$. For convenience and by analogy with optical terminology, we refer to the unequal-kick case as the ‘chirped’ or cdw-QKR. $N = 3$ is the minimum number needed to break time-reversal invariance: $N = 2$ in this system gives no transport. Larger numbers ($N > 3$) do give transport but have the effect of increasing break-times, which, as discussed below, we wish to keep small.

The upper graph in Fig.1 shows that, in both cases, the average energy of a classical ensemble of particles grows linearly with time t , ie $\langle p^2 \rangle \sim Dt$. Neglecting all correlations, it is approximated by $D \sim D_0 \sim K_{eff}^2/2$ where $K_{eff} = K \sqrt{1 + 4a^2}$. The Φ dependence appears in neglected correlations which in this case appear as products of Bessel functions [11]. For the standard QKR the corrections appear as oscillations in $D(K)$, with the maxima corresponding to the K 's for which accelerator modes are important. They were observed experimentally in [12]. We find that these corrections are unimportant for the cdw-QKR: the lowest order approximation gives a good fit from quite low values of K . The equal-kick case, the dw-QKR does need substantial corrections. In fact, since for the cdw-QKR phase-space periodicity in momentum is largely destroyed and indeed we find no evidence of accelerator modes; the dw-QKR is periodic in p and we find strong effects due to accelerator modes.

The *quantum* energy follows the classical trend but then saturates to a constant energy when $\langle p^2 \rangle \sim L^2$, where L is the localization length, after the break-time t^* . The break-time is substantially longer however (typically ~ 3 times) in the chirped case relative to the dw-QKR. We find that t^* grows as N . The figure shows that there is no net momentum in the $T = 1$ case and, asymptotically, $\langle p \rangle \simeq 0$. However, for the chirped case, for $t > t^*$, in general we have $\langle p \rangle \sim cst$. A meaningful way to quantify the asymmetry is a re-scaled momentum $p_L = \langle p \rangle / L$ which also tends to a constant for $t > t^*$ (eg $p_L \simeq 1/8$ in Fig. 1b for $\Phi = 0$.) Taking $\Phi = \pi$ reverses the symmetry of $V(x)$ and the direction of motion relative to $\Phi = 0$. Intermediate values of Φ

typically give $\langle p \rangle$ within these extremes. The experiments in [3] measured the momentum distribution of a cloud of atoms and observed the hallmark of DL : a triangular form of the logarithm of the momentum distribution $N(p)$. Fig 1(c) (upper) shows this is also the case for the dw-QKR. However, for the chirped case, the corresponding distribution is evidently asymmetric.

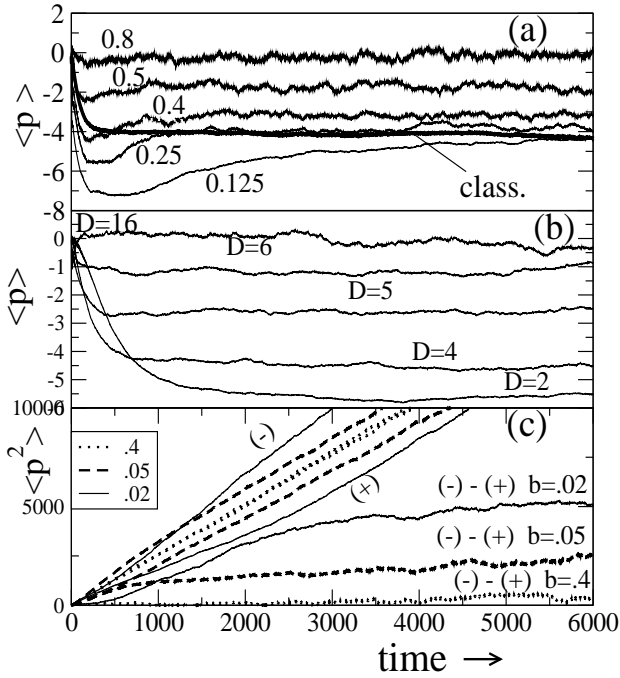


FIG. 2: Behaviour of the cdw-QKR. The results were obtained from quantum wavepackets and classical trajectories. Both the classical and quantum $\langle p \rangle$ reach a constant value after a finite time (t^* and t_r respectively). (a) Graph showing that the quantum ratchet transport is very sensitive to \hbar if the quantum wavepacket localizes before the classical wavepacket reaches t_r . The values of \hbar , (0.8 \rightarrow 0.125) are indicated. $K = 1.6, a = 1/2, N = 3$ (hence $D \sim 2.5$) and $b = 0.1$. The asymptotic quantum $\langle p \rangle$ increases with \hbar and ‘catches’ up with the classical results for $\hbar \sim 0.25$. (b) Evolution of $\langle p \rangle$ for a classical wavepacket (500,000 particles with a gaussian random distribution in x, p , of width $\sigma = 1.5$ for $b = 0.05$ but different D). The classical net momentum increases and then saturates after a classical saturation time $t_r \sim 1/(Db^2)$. (c) The effect of different classical diffusion rates ($D^+(t, b), D^-(t, b)$): $\langle p^2 \rangle$ is evaluated separately for positive and negative momenta for a cloud of classical particles with $D \sim 2.5$ and different b . We see that the growth in $\langle p^2 \rangle$ shows a divergence from linear growth which, for small $b\sqrt{\langle p^2 \rangle}$, is similar in magnitude but opposite in sign for the negative and positive components. The + and - indicate $\langle p^2 \rangle^+, \langle p^2 \rangle^-$ respectively. One sees that if $t > t_r$ then $D^+ \sim D^- \sim D \sim 2.5$. The lower graphs show $\langle p^2 \rangle^{(-)} - \langle p^2 \rangle^{(+)}$ (for these parameters, $D^- > D^+$) and show the $t_r \propto 1/b^2$ dependence.

The form for the first moment of $N(|p|)$ shows most clearly the source of the non-zero average of p . The dw-

QKR is symmetric. The cdw-QKR distribution, shows a substantial asymmetry. These asymptotic ‘frozen’ distributions are insensitive to changes in the starting position in x . We have investigated this effect for a range of different K, \hbar and a .

In Figs. 2a and 2b we show *both* quantum and classical net momenta $\langle p \rangle$ increase in magnitude, then saturate to a constant value after a finite time $\sim t^*$ in the quantum case or a ‘classical ratchet’ timescale t_r in the classical case. But they show other very interesting and surprising features. The quantum dependence on \hbar is shown in Fig. 2a. The $\langle p_{qm} \rangle$ are negligible for $\hbar > 1$ but increase rapidly with decreasing \hbar , up to $\hbar \sim 0.25$. This is important for any experiment : for these parameters, ($D \sim 2.5, b = 0.1$) an experiment with $\hbar_{eff} \sim 0.8$ would show little asymmetry, but just halving \hbar_{eff} to ~ 0.4 would show substantial asymmetry. Beyond $\hbar \sim 0.4$, $\langle p_{qm} \rangle$ is comparable to the saturated classical value. But since the most experimentally ‘detectable’ ratchet is one which maximizes the asymmetry in Fig.1(d), this means maximizing a re-scaled momentum $p_L = \langle p_{qm} \rangle / L$, so there is no advantage in reducing \hbar much below ~ 0.4 since $L \sim \hbar^{-1}$.

Fig 2b shows that, for a given b ($b = 0.05$ in this graph), the classical saturation time falls with increasing D . The fact that $\langle p_{cl} \rangle$ saturates at all is surprising: after all, the ensemble of classical trajectories is continually expanding and exploring new phase-space regions corresponding to higher momenta. Hence specific dynamical features such as partial barriers (cantori) do not account for this ratchet effect, though we find ‘scars’ of cantori do affect the detail of $N(p)$.

We solve the classical dynamics of the dw-QKR with the usual map, $x_{i+1} = x_i + P_i$; $P_{i+1} = P_i - V'(x_{i+1})$ for the i -th kick. For the chirped case, however, we have a 3-kick map (we consider $N = 3$ here but the analysis for $N > 3$ is qualitatively similar). We consider the first kick of the n -th cycle:

$$x_{n1} = x_{n0} + P_{n0}(1 + b) \quad (0.2)$$

$$P_{n1} = P_{n0} - V'(x_{n0} + P_{n0}(1 + b)) \quad (0.3)$$

The effect of the chirping is to allow the free evolution to proceed for an additional distance $\delta_1 = P_{n0}b$. The second kick has corresponding $\delta_2 = 0$ and the third kick has $\delta_3 = -P_{n2}b$. Since b is a small number, this represents a small perturbation at the start of the evolution of the cloud and to first order, for the first kick,

$$P_{n1} = P_{n0} - (V'(x_{n0} + P_{n0}) + P_{n0}bV''(x_{n0} + P_{n0})) \quad (0.4)$$

In general, if we work out the change in $\langle p^2 \rangle$ for successive kicks in the standard map we obtain a diffusion rate D which is the same (after the first few kicks) whether we average the momentum from $0 \rightarrow \infty$ or from $0 \rightarrow -\infty$. Both the zero-th order contribution $K^2/2$ as

well as higher corrections (such as those, for example, involving correlations between the i -th kick and the $(i+2)$ -th kick) are even in p and insensitive to the sign of p . However, in the cdw-QKR case, if we can make the perturbative expansion above, we now have correlations which depend on the sign of p and which scale with b .

For our classical ratchets, we calculated -separately- $\langle p^2 \rangle^{(-)}$ for those particles with $p < 0$ and $\langle p^2 \rangle^{(+)}$ for those with $p > 0$. The results are shown in Fig. 2c for $D_0 \sim 2.5$ and different b . They are quite striking : $\langle p^2 \rangle^{(-)}$ and $\langle p^2 \rangle^{(+)}$ separate gradually, more or less symmetrically, about the line $\sim 2.5t$, but beyond a certain time they run parallel to each other and their slopes become equal with $D^{(+)} \sim D^{(-)} \sim 2.5$. In the lower part of Fig. 2c we plot the actual difference $\langle p^2 \rangle^{(-)} - \langle p^2 \rangle^{(+)}$ for each b since this shows the saturation effect more clearly.

The saturation time t_r is very important since then the classical ratchet speed reaches its maximum and for $t > t_r$, $\langle p_{cl} \rangle \sim cst$. We identify it as a point far enough from where we can make the small angle perturbative approximation above. This will happen when $b\sqrt{\langle p^2 \rangle^{(+)}} \sim \pi$ for the positive component and $b\sqrt{\langle p^2 \rangle^{(-)}} \sim \pi$ for the negative component. For an order of magnitude estimate of the mean timescale involved, we take $b\sqrt{Dt} \sim \pi$. Hence we obtain $t_r \sim \frac{\pi^2}{Db^2}$.

Numerically, we estimate $t_r \sim \frac{5}{Db^2}$ which is not inconsistent with the above. This explains the counter-intuitive behaviour that the larger deviation from period-one kicking (ie the larger b), give a smaller ratchet effect. Though the perturbation scales as b , the time for which it is important scales as b^{-2} . So Fig. 2c shows that $b = 0.4$, which saturates at ~ 10 kicks, gives $\langle p \rangle \sim 0$ while $b = 0.02$, which saturates at ~ 5000 kicks, gives a very large asymmetry.

For the standard map/QKR there is a well-known relation between the quantum localization length and the classical diffusion constant: $L \sim \frac{\alpha D}{\hbar}$, where the constant α was found to be $1/2$ [13]. The $N = 3, b = 0.1$ cdw-QKR takes a modified proportionality constant, ie $L \sim \frac{3.5D}{\hbar}$. We have found this by fitting DL forms to a set of quantum distributions $N(p)$ corresponding to different D and \hbar . For large p , the distribution is well approximated by the DL exponentially localized profile.

In Fig. 3a we plot a set of calculated L (which range from $L \sim 10 - 80$) against D for $\hbar = 1/2$ together with the line corresponding to $L = \frac{3.5D}{\hbar}$. The agreement is excellent. From $L^2 \sim Dt^*$ we obtain $t^* \sim 12D/\hbar^2$.

In Fig. 3b, for the quantum distributions in Fig 3a, we have also plotted the net momenta as a functions of D , together with their classical equivalents, obtained from an ensemble of 500,000 classical particles. We see that the classical $\langle p \rangle$ fall monotonically with D , apart from fine structure which we attribute to cantori. The quantum results however, for low D , are much smaller than the classical values but increase in magnitude until there is a ‘cross-over’ point at $D \sim 3$, after which they are

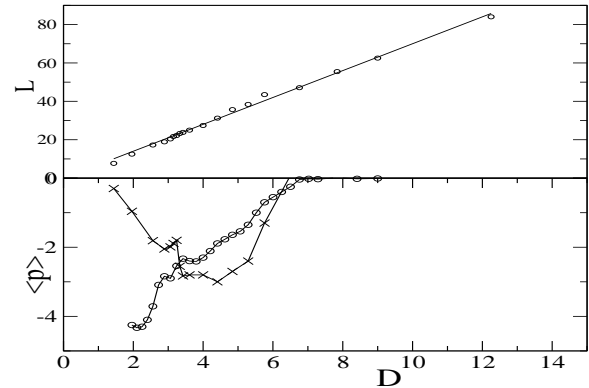


FIG. 3: (a) Relation between classical diffusion rate D and the quantum localization length L for the cdw-QKR. The solid line corresponds to $L = \frac{3.5D}{\hbar}$. (b) Average momentum plotted against D for a quantum wavepacket (crosses) and a classical ‘gaussian wavepacket’ (circles). The graph illustrates the fact that if the quantum break-time is too short (low D) the quantum momentum is small, but catches up with the classical momentum at $t^* \sim t_r$.

much closer to the classical values.

We do not expect perfect agreement with the classical results for $\hbar = 1/2$; a cleaner comparison might be obtained for smaller \hbar , but this might be harder to achieve in an experiment. We estimate the quantum break-time at the cross-over $t^* \sim 12D/\hbar^2 \sim 150$ kicks. The ratchet time $t_r \sim 5/(Db^2) \sim 160$ kicks. Such good agreement is somewhat fortuitous, since there are larger uncertainties in the timescales. Nevertheless it does provide us with a useful guide for the best parameters for an experiment.

So one of our key results is that the requirement $t^* \sim t_r$ implies that we need $Db/\hbar \sim 1$. This is a necessary but not sufficient condition to ensure the best cold-atom ratchet. Clearly the L values should be experimentally plausible $L \sim 10 - 100$, so this places a constraint on D/\hbar . Equally, for a good classical ratchet, b should be small ie $b < 0.2$.

Although the values of D considered may be small compared with those of the standard map, we find the chirped dw-QKR is much more chaotic at a given value of D . There are no remaining stable islands visible on an SOS at the parameters corresponding to Figs 1-3.

In conclusion, we have found a mechanism for a generic, completely chaotic Hamiltonian ratchet. But much remains to be done, such as considering the effect of the partial loss of coherence in the experiment or the effect of the finite duration of the experimental kicks. Though transport appears as a general sign-dependent correction to the classical diffusion rate, the role of specific dynamical effects such as desymmetrization of Levy flights [8] must be investigated.

We thank Prof. S Fishman for helpful advice. N.H

and M.I acknowledge EPSRC studentships. The work was

supported by EPSRC grant GR/N19519.

- [1] G. Casati, B.V. Chirikov, Izraelev F.M., and J. Ford in "Lecture notes in Physics", Springer, Berlin **93** , 334 (1979).
- [2] S. Fishman, D.R. Grempel, R.E. Prange, Phys. Rev. Lett. **49**, 509 (1982).
- [3] F.L. Moore, J.C. Robinson, C.F. Bharucha, Bala Sundaram, and M.G.Raizen, Phys. Rev. Lett. **75**, 4598 (1995).
- [4] C. Mennerat-Robilliard, D. Lucas, S.Guibal et al, Phys. Rev. Lett. **82**, 851 (1999).
- [5] We thank Dave Meacher for explaining possible experiments with driven double-well lattices :two phase-locked optical-lattices seem to offer the best possibility of an atomic kicked ratchet.
- [6] F.Julicher, A. Adjari and J.Prost, Rev. Mod. Phys., **69**, 1269 (1997).
- [7] P. Reimann, M. Grifoni, and P. Hänggi, Phys. Rev. Lett. **79**, 10 (1997); P. Reimann and P. Hänggi, Chaos, **8**, 629 (1998).
- [8] S. Flach, O. Yevtushenko, Y. Zolotaryuk, Phys. Rev. Lett. **84**, 2358 (2000).
- [9] T. Dittrich, R. Ketzmerick, M.-F.Otto, and H. Schanz, Ann. Phys. (Leipzig) **9**,1 (2000); H. Schanz, M.-F.Otto, R. Ketzmerick T. Dittrich, Phys. Rev. Lett. **87**, 070601 (2001).
- [10] T. Cheon, P. Exner, P. Seba, preprint, cond-mat/0203241, 12 March 2002.
- [11] N. Hutchings et al, in preparation.
- [12] B.G. Klappauf, W.H. Oskay, D.A. Steck, and M.G.Raizen, Phys. Rev. Lett. **81**, 4044 (1998).
- [13] D. L. Shepelyansky Phys. Rev. Lett. **56**, 577 (1986).